processes

MDPI

Article

Development of Geopolymer Mortars Using Air-Cooled Blast Furnace Slag and Biomass Bottom Ashes as Fine Aggregates

Yolanda Luna-Galiano *, Carlos Leiva Fernández, Rosario Villegas Sánchez and Constantino Fernández-Pereira

Departamento de Ingeniería Química y Ambiental, Escuela Técnica Superior de Ingeniería, Universidad de Sevilla, Camino de los Descubrimientos s/n, 41092 Seville, Spain; cleiva@us.es (C.L.F.); rvillegas@us.es (R.V.S.); pereira@us.es (C.F.-P.)

* Correspondence: yluna@us.es; Tel.: +34-954481180

Abstract: The aim of this study is to compare the mechanical and physical properties of different geopolymer mortars made with granulated blast furnace slag as a geopolymer source material, NaOH (8 M) as the activating solution, and three different types of fine aggregates (air-cooled blast furnace slag, biomass bottom ashes, and silica sand). The samples were made with an aggregate/geopolymer ratio of 3/1, and physical (density and mercury intrusion porosimetry), mechanical (compressive and flexural strength), and acid attack resistance were determined. When air-cooled blast furnace slag is used, the mechanical and acid attack properties are improved compared with silica sand and biomass bottom ashes because of the existence of amorphous phases in this slag, which increase the geopolymer reaction rate despite the particle size being higher than other aggregates. It can be highlighted that the use of ACBFS as a fine aggregate in geopolymer mortars produces better properties than in cement Portland mortar.

Keywords: geopolymer mortar; air-cooled blast furnace slag; olive pomace bottom ash; mechanical properties; porosity; leaching; acid attack resistance

check for updates

Citation: Luna-Galiano, Y.; Leiva Fernández, C.; Villegas Sánchez, R.; Fernández-Pereira, C. Development of Geopolymer Mortars Using Air-Cooled Blast Furnace Slag and Biomass Bottom Ashes as Fine Aggregates. *Processes* **2023**, *11*, 1597. https://doi.org/10.3390/pr11061597

Academic Editor: Antoni Sánchez

Received: 24 March 2023
Revised: 19 May 2023
Accepted: 20 May 2023
Published: 23 May 2023

1. Introduction

The European Union presents the circular economy as a viable alternative to the prevailing model of production and consumption worldwide, especially in developed countries or in those where excessive means of production are used, which encourage compulsive and sometimes unnecessary consumption, blurring the idea of acquiring goods and services for their necessity [1].

This new paradigm requires a significant shift in current production and consumption systems. The shift must be toward regenerative systems that are designed to conserve the value of resources (materials, water, soil, and energy) and products while exponentially diminishing raw material and energy inputs. This will reduce waste generation and negative impacts, hence decreasing negative externalities for the environment, climate, and human health [2].

The construction sector is one of the main polluters. For example, the cement industry is responsible for the emissions of 2 gigatons of carbon dioxide (CO_2) per year, which is more than 5% of the total world emissions, and it is expected that by 2050, the emissions will be 5 gigatons [1]. There are numerous lines of investigation researching the replacement of cement with geopolymers [3]. Geopolymerization is a term coined by Joseph Davidovits in the 1980s to designate synthetic inorganic polymers of aluminosilicates resulting from the chemical reaction known as geopolymerization [4]. Geopolymers have the advantages of low CO_2 emissions during production, high chemical and thermal resistance, and satisfactory mechanical properties, all at room temperature and at extreme temperatures. The geopolymerization reaction takes place under highly alkaline conditions between an aluminosilicate powder and an activating solution (alkaline hydroxide and/or alkaline

silicate) at ambient or slightly above ambient conditions (<60 °C), to obtain a new synthetic alkaline aluminosilicate of a polymeric chain structure.

Many wastes (coal fly ashes, blast furnace slag, construction and demolition wastes, municipal solid waste incineration ashes, metallurgical and mining waste, etc.) [5–9] have been studied as raw materials for the manufacturing of geopolymeric materials such as concrete, mortars, building components, insulation, and fire-resistant coatings [10–13].

Slags developed during the manufacturing of pig iron are referred to as "blast furnace" slags and are produced by the smelting of various fluxes mixed with gangue minerals. The raw material quality, as well as the design and operation, determine the quality and quantity of slag. Several types of slags are produced. Granulated blast furnace slag, air-cooled blast furnace slag, expanded or foamed slag, and pelletized slag are the various names for these products [14].

Granulated BFS is obtained by cooling the liquid slag by dropping it on a powerful jet of cold water, thereby making it expand, and using the water jet as a transport vehicle to the decantation basins. During this process (granulation), the slag vitrifies. The principal use of granulated blast furnace slags is for cement production [15,16], but GBFS can also be used as a raw material to obtain geopolymers [7,17], showing good physical and mechanical properties.

Air-cooled blast furnace slag (ACBFS) is also a material derived from iron and steel production, which is obtained by slow cooling of the liquid slag in large facilities. The material crystallizes, forming different components, leaving only a small part in a glassy state. The principal uses of this material are cements with soil-cement additions [18], geopolymers [19], base layers of roads [20], and sound absorption materials [21]. Previous studies [15] have analyzed the use of ACBFS as a fine aggregate, but the results are worse than for natural aggregates. In 2016, 430,000,000 tons of slag were produced, 66% of which were granulated blast furnace slags and 34% air-cooled blast furnace slags [14].

Olive pomace is used as biomass because of its high energy content and low cost; around 30% of it is used to create power. In Spain, the combustion of olive pomace produces more than 50,000 tons of ash each year [22].

Bottom and fly ash are two types of ash created during the combustion process of solid fuel. Bottom ash is created on the grate in the boiler's initial combustion chamber, and it presents a higher percentage of unburned biomass. Previous studies have used these bottom ashes in bricks [23,24], cement manufacture [25], road binders [26], geopolymers [27], fine aggregates in mortars [28], fire resistance materials [29], and fertilizers [30], but the percentage of recycling is very low.

Although ACBFS and olive pomace bottom ash (OPBA) has previously been used as sources of aluminum and silicon to produce geopolymers and as a fine aggregate for mortars using Portland cement, the results have not been promising [15,19,27,28]. The aim of this study is to compare the mechanical and physical properties of two types of geopolymeric mortars made with BFS as geopolymeric precursor, NaOH (8 M) as activating solution, and ACBFS and OPBA as fine aggregates. This work presents two important benefits: (1) the environmental benefit by means of the valorization of three wastes/byproducts in this construction material, fulfilling the European regulation regarding circular economy, and (2) the respective cost savings because of not landfilling these wastes.

2. Materials and Methods

2.1. Materials

Mortars were made with three fine aggregates and a geopolymer cement as the binder. The geopolymer cement is made by means of the activation of granulated blast furnace slag (BFS) with NaOH (8 M). The fine aggregates are standard silica sand, air-cooled blast furnace slag, and olive pomace bottom ash.

Both granulate (BFS) and air-cooled (ACBFS) blast furnace slag come from EDERSA (Gijón, Asturias, Spain). Biomass bottom ashes came from an energy generation process that uses only olive pomace in an inclined grill oven from Villanueva del Arzobispo (Jaén, Spain). Figure 1 shows an image of the four raw materials.

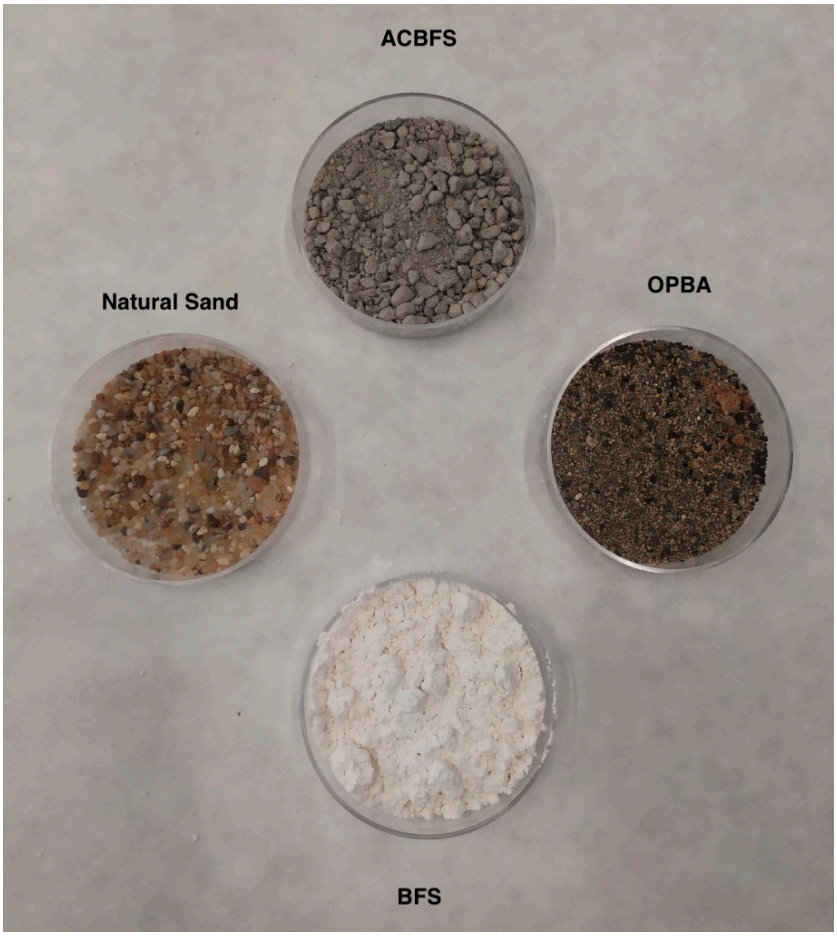

Figure 1. Solid wastes and natural silica aggregates.

The chemical composition of BFS and ACBFS is practically the same, as can be seen in Table 1. Both materials comprise four main components: lime, silica, alumina, and magnesia, which constitute more than 95%. The chemical composition of the slags varies depending on the steelmaking process employed and varies between 27–50% of SiO_2; 5–33% of Al_2O_3; 30–50% of CaO, and between 1–21% of MgO [19].

Table 1. Chemical composition, specific gravity, and loss on ignition of the materials.

Chemical Composition (% Weight)	BFS	Natural Aggregate	ACBFS	OPBA
CaO	43.46	0.59	42.14	16.5
SiO_2	35.82	86.5	34.76	45.4
Al_2O_3	11.60	5.83	9.12	10.4
MgO	7.59	0.13	6.06	5.0
SO_3	-	0.04	1.77	-
TiO_2	-	0.13	0.76	-
K_2O	0.36	2.37	0.54	17.2
Fe_2O_3	1.01	1.33	0.42	4.2
MnO_2	-	-	0.41	-
Na_2O	0.21	0.87	0.19	1.7
BaO	-	-	0.11	-
P_2O_5	-	0.07	-	-
MnO	-	0.03	-	-
Specific gravity (g/cm^3)	2.93	2.71	2.91	2.05
Loss on ignition (%)	1.47	1.34	1.49	9.30

According to EN 196-1 [31], natural silica fine aggregate (NA) (standard sand) is processed mainly from what used to be lakes and rivers where large silica sand sediments are found. SiO_2 exceeds 85% of its chemical composition.

As can be seen, CaO, SiO_2, Al_2O_3, and K_2O are the main components of olive pomace bottom ash (OPBA). In addition, OPBA presents a high unburned content, which leads to the particles presenting a low specific gravity.

The XRD analysis of BFS, ACBFS, and OPBA was carried out using a D8 Advance A25 instrument (BRUKER) (40 kV and 30 mA). The DIFFRAC-EVA software (BRUKER) was used for phase identification. The software works with a reference database ICDD PDF4.2022 version of JCPS. Phase identification and accurate quantitative phase analysis (amorphous and crystalline contents) are based on the reference intensity ratio (RIR) method [32,33]. Figure 2 shows the diffractograms of the three raw materials.

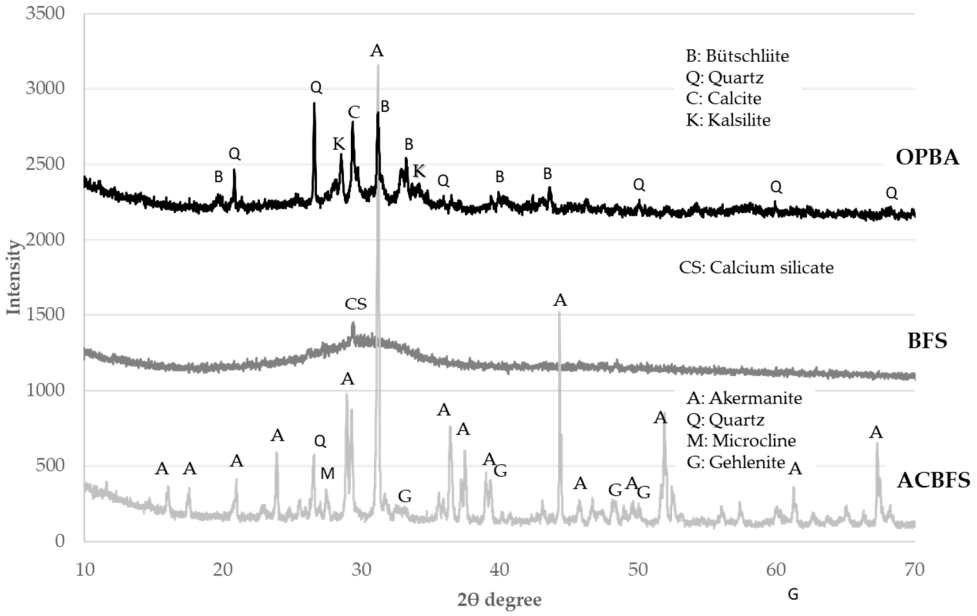

Figure 2. X-ray diffraction of BFS, ACBFS and OPBA.

Curves of BFS and OPBA were moved 1000 and 2000, respectively, from the real intensity to improve the visualization of the curves. The XRD pattern of BFS showed a broad peak in almost all 2θ ranges which is characteristic of an amorphous material (60.4%). BFS only presented a peak corresponding to calcium silicate. ACBFS presented an amorphous content of 20.5%. The main crystalline phases were akermanite, quartz, microcline, and gehlenite. OPBA showed an amorphous content of 39.6%. Quartz, bütschliite, calcite, and kalsilite were identified as the main crystalline phases. As can be seen, BFS has a large amount of vitreous content, which made it a perfect raw material for the geopolymerization reaction. On the other hand, ACBFS, which comes from the same process but with a slow cooling in the air, showed a lower content of vitreous phase than BFS.

The particle size was examined using a Mastersizer 3000 particle size analyzer. The particle size distribution of the three fine aggregates is depicted in Figure 3. OPBA presents a particle size between 0–1500 μm with an average particle size of 387 μm. NA presents a particle size between 250–1500 μm, with an average particle size of 680 μm while ACBFS presents a wider size range than SS (0–2000 μm), but with a slightly lower average particle size (660 μm) than NA. Previous research shows that BFS presents a smaller particle size (50–100 μm) compared to the three fine aggregates [16].

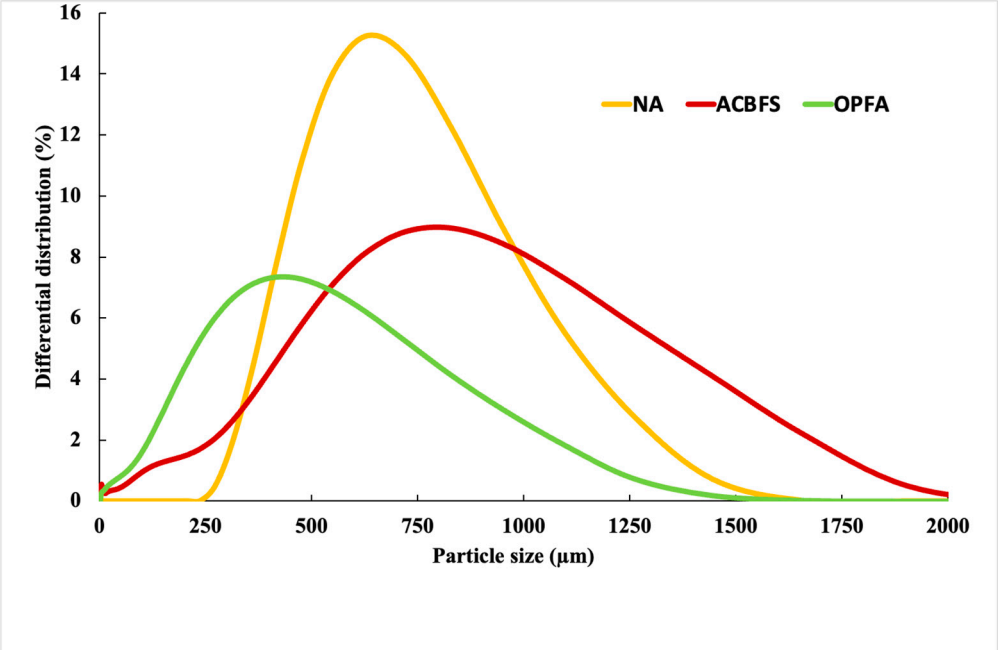

Figure 3. Particle size distribution of the fine aggregates.

2.2. Methods

2.2.1. Geopolymeric Mortar Preparation

Three different geopolymeric mortars were manufactured at room temperature using a mixer (KitchenAid). The solid phase (BFS and fine aggregates) was mixed for 4 min at low speed. Next, the liquid phase (activating solution, superplasticizer, and water) was added to the solid phase, and all materials were mixed for a further 10 min. Table 2 shows the different dosages. The geopolymer binder was prepared using BFS as the source material and NaOH 8 M as the activating solution. In all cases, a superplasticizer (SP) based on polycarboxylic ether-based superplasticizer (MasterEase 5025) was added. NaOH/BFS, fine aggregate/BFS, and SP/BFS ratios were kept constant in all the mortars. Previous tests were performed to calculate the accurate ratios of water to obtain a thixotropic material with the same workability, as can be seen in Table 3. Mixtures with OPBA required a higher H_2O/BFS ratio, due to the higher LOI content, lower specific gravity, and fine particle size, which increase the absorption of water during the mixing. Mixtures with SS showed the lowest H_2O/BFS ratio since SS presents the highest specific gravity (lower porosity).

Table 2. Ratios of geopolymeric mortars.

Fine Aggregates	NaOH/BFS	Fine Aggregate/BFS	SP/BFS	H_2O/BFS
M-NA	0.3	3	0.078	0.027
M-CBFS	0.3	3	0.078	0.168
M-OPBA	0.3	3	0.078	0.503

Table 3. Density and strength of mortars.

Fine Aggregates	Density (kg/m^3)	Compressive Strength (MPa)	Flexural Strength (MPa)
M-NA	2313 ± 24	17.6 ± 1.1	2.5 ± 0.2
M-CBFS	2316 ± 34	18.9 ± 0.9	2.7 ± 0.1
M-OPBA	1712 ± 15	14.9 ± 0.7	2.0 ± 0.1

The solid phase (blast furnace ash and fine aggregates) was mixed for 4 min in a mixing machine. Next, activating solutions SP and H_2O were added to the previous mixture and

mixed for 15 min. The resulting paste was placed in molds and was vibrated on the vibrating machine for 1.5 min. The setting time of the mortars was less than 15 h at room temperature, results were similar to other works [34], then, 24 h after their manufacture, the samples were unmolded, wrapped in transparent film, and left to cure for a total of 28 days at 20 °C.

2.2.2. Mortar Characterization

The density of the mortars was evaluated in accordance with EN 1936 [35] for samples cured for 28 days.

The pore size distribution in the range of 1 to 300 µm was studied using mercury intrusion porosimetry (MIP-PoreMaster 60GT). The surface tension was 480 mN/m, the contact angle was 140°, and the maximum pressure was 413 MPa.

After 28 days, flexural and compressive tests were performed on parallelepipeds 160 × 40 × 40 mm, using a Tinius Olsen-TO317EDG, in accordance with EN 1015-11 [36]. For these tests, 5 parallelepipeds of each mortar were used, and the 2 pieces after the flexural test (10 per composition) were subjected to compressive tests.

Resistance to acid attack is measured by evaluating the compressive strength of the samples after immersion in 1 M sulfuric acid and water for 15 days (Figure 4), in accordance with previous studies [37].

Figure 4. Samples in sulfuric acid.

For the test, four samples of each mortar were left to cure during a 28-day period. Two of the samples were immersed in 1 M sulfuric acid, while the other two were left out in the air. Acid samples were removed after 15 days. Then, they were dried at room temperature for 2 days, and compressive strength was determined.

2.2.3. Leaching Study

According to EN 998-2 [38], mortars require the study of emissions of dangerous substances, using standardized European tests and considering the different existing national and regional provisions, although the said standard does not have any specific tests or limits that must be met.

There are more than 55 different leaching tests for different conditions and materials. Leaching tests can be classified mainly as static, dynamic, and tank tests.

In static tests, the leaching solution is a single addition that is not updated during the test. The most used batch leaching tests are EN 12457-4 [39] and TCLP [40].

The leaching solution is recovered during dynamic experiments. This approach is unsuitable for monolithic materials, such as cement-based materials, unless the material size is reduced to the standard size required before testing.

The tank test method involves rinsing the monolithic material in reagent water in a tank. The most common tank tests are NEN 7345 [41] and EPA-1315 [42] and require more than 60 days of testing.

In static tests, the leaching solution is a single addition which is not updated during the test. EN-12457-4 [39] is the most frequently used leaching test in Europe, and it is used to classify wastes in accordance with the EU Landfill Directive [43]. The test is quite basic. It is based on a single stage leaching at a liquid/solid ratio of 10/1 for materials with particle size distributions less than 10 mm. The liquid/solid mixture was rotated at 15 rpm for 24 h. This study made use of deionized water. The Research, Technology, and Innovation Center of the University of Seville (CITIUS) provided an ICP spectrometer (Agilent Technologies, Madrid, Spain). Each leaching was subjected to two leaching tests.

Furthermore, this test is utilized in various European national and regional leaching regulations to evaluate waste use in construction applications. For example, Portugal [44], Italy [45], and some Spanish regions (Cantabria [46] and Basque Country [47]) have imposed leaching limits for the valorization of wastes as part of construction materials based on the results of this test.

3. Results and Discussion

3.1. Physical and Mechanical Properties

In Table 3, physical and mechanical properties (density, compressive, and flexural strength) are shown. With respect to density, geopolymer mortars prepared with NA and ACBFS presented similar values. Geopolymer mortar prepared with OPBA presented a very low density (almost half compared with the other two).

To explain the results, porosity and pore size distribution were also analyzed. Porosities of geopolymer mortars are: 0.5 (M-NA), 0.8 (M-ACBFS), and 3.22 mL/g (M-OPBA). Figure 5 shows the pore size distribution of the geopolymer mortars. M-OPBA presented a high proportion of sorption pores (<0.1 µm) due to the presence of hydrated phases [48] and the internal porosity of these bottom ashes because of the high quantity of unburned matter (Table 1) present in the OPBA aggregate. Capillary pores are also visible in the graph (ranging in size from 0.1 to 100 µm). They are the pores generated within the binder and in the aggregate/binder interface. Water movement causes primary porosity due to absorption into the surrounding masonry unit or evaporation to the air. Because of its high water/solid ratio, M-OPBA has more capillary holes due to its high-water requirement (Table 2). For these reasons, the M-NA mortar shows the lowest number of capillary pores.

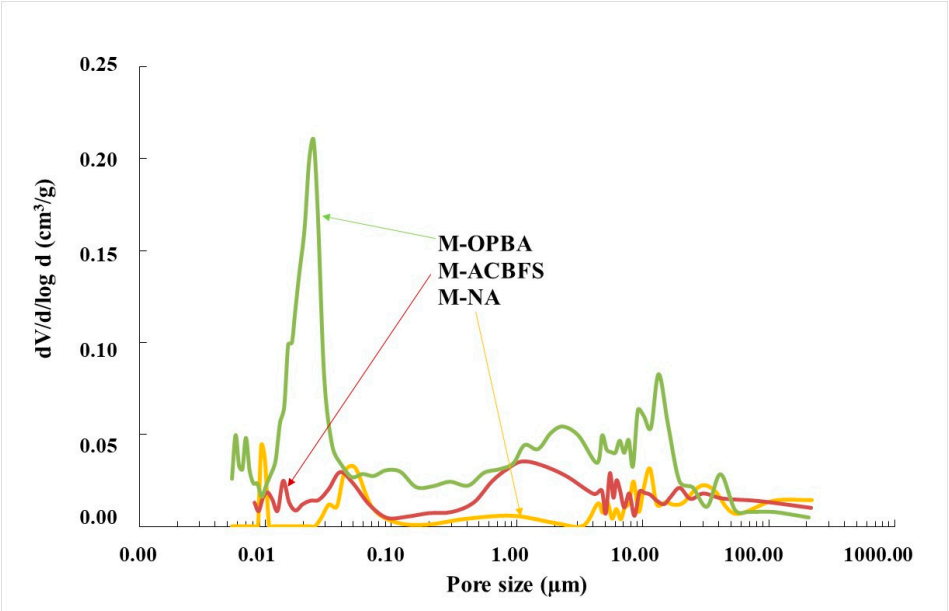

Figure 5. Pore size distribution of the mortars.

Coarse pores present sizes higher than 100 μm. Aggregates with high particle sizes produce higher pores between particles. Consequently, M-OPBA mortars present a lower coarse pore content compared with M-ACBFS and M-NA.

M-ACBFS mortar presented the highest compressive strength values (slightly higher than M-NA and much higher than M-OPFA).

XRD of the three mortars was carried out and diffractograms are presented in Figure 6.

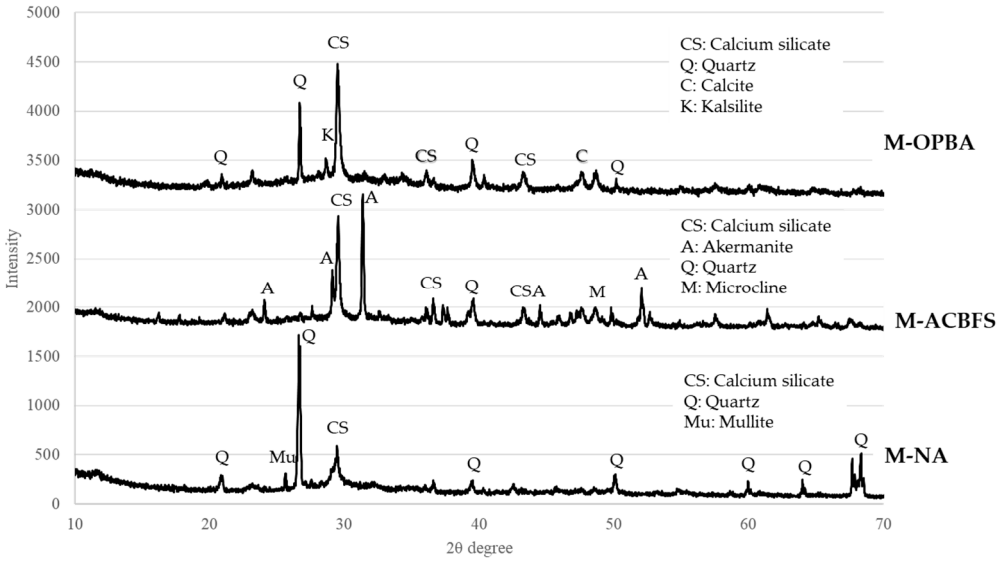

Figure 6. Mortars diffractograms.

Curves of M-ACBFS and M-OPBA were moved 1700 and 3000, respectively, from the real intensity to improve the visualization of the curves. As can be seen, calcium silicate appears in all curves; the crystalline phase comes from the BFS. Calcite, quartz, and kalsilite from the OPBA stayed in the M-OPBA. However, the Bütschliite completely disappeared. Akermanite, quartz and, microcline from the ACBFS remained in the M-ACBFS (reduction of the akermanite peak is important) and the gehlenite disappeared. M-NA presented peaks of quartz and mullite, which comes from the natural aggregate (standard sand). Amorphous content of M-NA, M-ACBFS, and M-OPBA was determined by DIFFRACT.EVA software and the results were 34.2, 36.3, and 41.9%, respectively. Considering that the amorphous content in the M-NA (34.2%) is due to the BFS attack (NA was contacted with the activating solution and no reaction was displayed (wet sand behavior was observed)) and comparing the amorphous content of the three mortars (M-ACBFS = 36.3% and M-OPBA = 41.9%), it can be confirmed that the aggregates ACBFS and OPBA have been attacked during the geopolymerization reaction, contributing to the development of the amorphous phase of the final material.

Although M-ACBFS presented higher porosity than M-NA, the CS of M-ACBFS was slightly higher due to the greater amorphous content of M-ACBFS lead by the contribution of BFS and ACBFS (materials with amorphous content of 60.4 and 20.5%, respectively) to the geopolymerization reaction, which creates a final mortar with a higher content of geopolymer gel and better CS. In addition, BFS and ACBFS are similar materials with the same source; therefore, compatibility and adhesion between the geopolymer gel, the unreacted BFS and ACBFS, could be right to improve the CS [19].

M-OPBA mortars presented the worst mechanical properties. This mortar showed the highest amorphous content (41.9%) of the three mortars; therefore, the contribution of OPBA to the amorphous content of the M-OPBA is greater than the ACBFS and NA in their respective mortars. However, this higher contribution does not correspond with the CS results. This could be due to the effect of the smallest particle size and unburned content of OPBA, which produces greater requirements of water to obtain a workable material, with a final result of a low-density mortar with a lower CS.

According to EN 998-2 [38], M-NA and M-ACBFS could be classified as M-15 to be used as masonry mortars, and M-OPBA is slightly below M-15 and can be classified as M-10. On the other hand, all mortars present a compressive strength higher than 12.4 MPa at 28 days, and they can be classified as type S mortars according to ASTM C270 for masonry mortars [49].

The flexural strength followed the same trend as density and compressive strengths. The mortars made with NA and ACBFS, which contained less water, obtained the highest flexural strength results. On the other hand, the OPBA mortar presents a high porosity; therefore, the flexural test showed the worst results. As previously mentioned, the use of ACBFS produced a higher geopolymerization process and slightly increased the flexural strength.

3.2. Acid Attack Test

Compressive strength results after air contact and acid immersion for a further 15 days are shown in Figure 7. All the compressive strength results after the acid attack are lower than air. The main effect of the sulfuric acid attacks in the matrix was the generation of gypsum inside the pores and all around the sample (Figure 8), which causes pore spalling and results in worse mechanical properties for all the mortars [26]. This decrement is directly related to the macropores present in the mortars; M-OPBA presents a high proportion of macropores (Figure 5) and presents a higher percentage of diminution (41% of reduction), while M-NA presents a low amount of macropores, and its diminution is lower (23% of reduction).

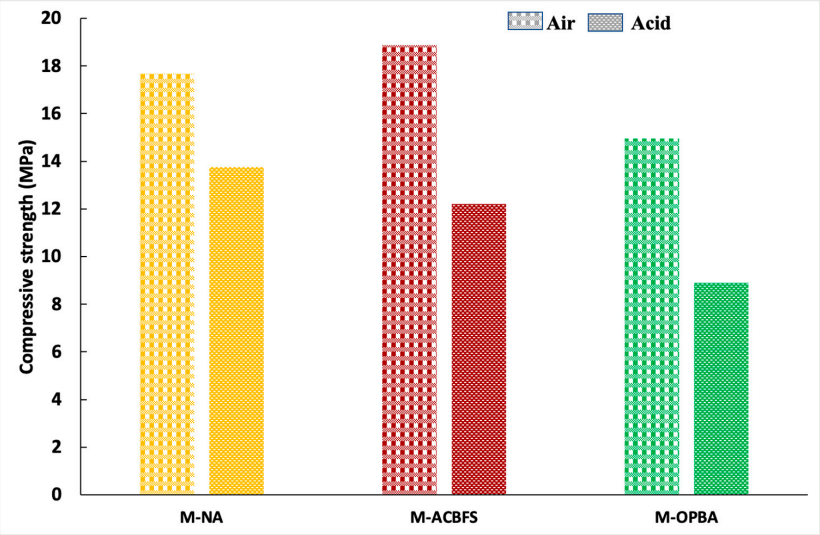

Figure 7. Compressive strength after acid attack.

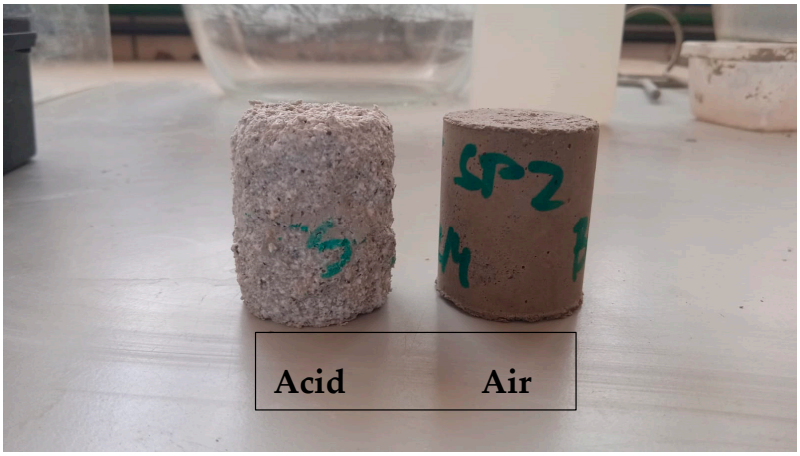

Figure 8. M-ACBFS after immersion in sulfuric acid and air for 15 days.

3.3. Leaching Study

EN-12457-4 [39] has been used to characterize the leaching behavior of the different solid materials. According to the EU Landfill Directive [41], this test is used to classify wastes [43].

Table 4 shows the results of the leaching test of BFS, ACBFS, OPBA, and NA. Three categories are defined by the Landfill Directive: inert, non-hazardous, and hazardous wastes. Results show that ACBFS, BFS, and NA can be considered an inert waste. Because the values of Se, Sb, and Ni are higher than inert limits but lower than non-hazardous standards, OPBA can be classified as non-hazardous waste.

Table 4. Leaching results of different solid materials of EN 12457-4 (mg/kg, dry basis).

	BFS	NA	OPBA	ACBFS	Inert Waste	Non-Hazardous Waste	Hazardous Waste
As	<0.2	<0.2	1.8	<0.2	0.5	2	25
Zn	<0.25	<0.25	<0.25	<0.25	4	50	200
V	0.19	-	-	0.16	-	-	-
Sn	<0.25	-	-	<0.25	-	-	-
Se	<0.04	<0.04	0.4	0.07	0.1	0.5	7
Sb	<0.05	<0.05	0.2	<0.05	0.06	0.7	5
Pb	<0.2	<0.2	9.3	<0.2	0.5	10	50
Ni	<0.05	<0.05	1.3	<0.05	0.4	10	40
Mo	<0.2	<0.2	1.8	<0.2	0.5	10	30
Hg	<0.01	<0.01	<0.01	<0.01	0.01	0.2	2
Cu	<0.1	<0.1	6.7	<0.1	2	50	100
Cr	<0.1	<0.1	<0.1	<0.1	0.5	10	70
Co	<0.02	<0.02	<0.02	<0.02	-	-	-
Cd	<0.02	<0.02	<0.02	<0.02	0.04	1	5
Ba	13.1	0.82	0.3	0.7	20	100	300

Portugal [44] and Italy [45] have national requirements, whereas Spain (Cantabria [46] and Basque Country [47]) present regional regulations for waste recycling in construction materials in accordance with the results of EN 12457-4. Table 5 shows the comparison of the results with the different international and regional requirements.

Table 5. Leaching results of EN 12457-4 compared with different international and regional requirements (mg/kg, dry basis).

Element	Portugal [43]	Italy [44]	Cantabria [45]	Basque Country [46]	BFS	OPBA	ACBFS
Zn	4	0.03	4	1.2	<0.25	<0.25	<0.25
V	-	-	-	1.3	0.19	-	0.16
Sn	-	-	-	-	<0.25	-	<0.25
Se	0.1	0.1	0.1	0.007	<0.04	0.4	0.07
Sb	0.06	-	0.06	-	<0.05	0.2	<0.05
Pb	0.5	0.5	0.5	-	<0.2	9.3	<0.2
Ni	0.4	0.1	0.4	0.8	<0.05	1.3	<0.05
Mo	0.5	-	0.5	1.3	<0.2	1.8	<0.2
Hg	0.01	0.01	0.01	-	<0.01	<0.01	<0.01
Cu	2	0.5	2	-	<0.1	6.7	<0.1
Cr (total)	0.5	0.5	0.5	2.6	<0.1	<0.1	<0.1
Co	-	-	-	-	<0.02	<0.02	<0.02
Cd	0.04	0.05	0.04	0.009	<0.02	<0.02	<0.02
Ba	20	10	20	17	13.1	0.3	0.7
As	0.5	0.5	0.5	-	<0.2	1.8	<0.2

In Portugal, waste recycling is permitted as long as the limit for inert waste [42] in waste components is not exceeded. According to Portuguese law, BFS and ACBFS could be reused, but not OPBA. According to the Italian requeriments [45], OPBA cannot be used

due to excessive As, Mo, Pb, Se, Ni, Sb, and Cu levels. BFS has a greater Ba leaching content, whereas ACBFS matches the standards of the Italian law.

In Spain, there are no specified national limitations for heavy metals leaching of wastes as raw materials. Nonetheless, there is regional legislation based on EN 12457-4 results, that allows us to determine whether a waste can be recycled in construction applications, such as Cantabria and Basque Country legislations. BFS and ACBFS can be recycled in construction materials in Cantabria and Basque Country under these conditions. Most of the metals in OPBA leaching exceed the Cantabria and Basque Country limits.

4. Conclusions

The results of some physical, leaching, and mechanical properties of two different recycled aggregates, air cooled blast furnace slag and olive pomace bottom ash in geopolymeric mortars has been analyzed.

Although OPBA shows amorphous content which is slightly activated by the alkaline solution, as can be observed with the amorphous content of the M-OPBA, in the M-OPBA prevails the effect of the smallest particle size and unburned content of the OPBA, which produces greater requirements of water to obtain a workable material, with the final result of a low-density mortar with lower CS.

Regarding mechanical properties, geopolymeric mortars with ACBFS have 7% more compressive and flexural strength than those made with OPBA and even with NA. This result could be due to two reasons. On one hand, ACBFS presents an amorphous content, which, although it is lower than BFS, it is significant enough to participate in the geopolymerization reaction. On the other hand, chemical similarities between BFS and ACBFS could improve the compatibility and adhesion between the geopolymer paste, the unreacted BFS and ACBFS, upgrading the final mechanical properties.

Leaching studies have also been performed to determine the environmental safety use of these wastes. According to those findings, OPBA has leaching values greater than several Spanish, Portuguese, and Italian criteria, but the use of ACBFS has not presented any leaching problems.

According to EN 998-2 [38], M-NA and M-ACBFS could be classified as M-15 to be used as masonry mortars while, as M-OPBA strength is slightly below the M-15 limit, it must, therefore, be classified as M-10.

Author Contributions: Conceptualization, Y.L.-G. and C.F.-P.; methodology, C.L.F.; validation, Y.L.-G. and C.L.F.; formal analysis, Y.L.-G., C.F.-P., C.L.F. and R.V.S.; investigation, Y.L.-G. and C.L.F.; resources, C.F.-P.; writing—original draft preparation, Y.L.-G. and C.F.-P.; writing—review and editing, Y.L.-G. and R.V.S.; supervision, C.F.-P.; project administration, Y.L.-G. All authors have read and agreed to the published version of the manuscript.

Funding: The Junta de Andalucia's (Spain) Ministry of Development, Infrastructure, and Territory Planning (grant number: US.20-14) and the Spanish National Plan 2017–2020 under grant number: PID2019-110928RB-C33 provided funding for this project.

Data Availability Statement: Data available on request due to restrictions eg privacy or ethical.

Acknowledgments: CITIUS-University of Seville Innovation, Technology and Research Centre.

Conflicts of Interest: The authors declare no conflict of interest.

References

1. Peceño, B.; Bakit, J.; Cortes, N.; Alonso-Fariñas, B.; Bonilla, E.; Leiva, C. Assessing Durability Properties and Economic Potential of Shellfish Aquaculture Waste in the Construction Industry: A Circular Economy Perspective. *Sustainability* **2022**, *14*, 8383. [CrossRef]
2. Alonso-Fariñas, B.; Rodríguez-Galán, M.; Arenas, C.; Torralvo, F.A.; Leiva, C. Sustainable management of spent fluid catalytic cracking catalyst from a circular economy approach. *Waste Manag.* **2020**, *110*, 10–19. [CrossRef]
3. Lu, X.; Liu, B.; Zhang, Q.; Wen, Q.; Wang, S.; Xiao, K.; Zhang, S. Recycling of Coal Fly Ash in Building Materials: A Review. *Minerals* **2023**, *13*, 25. [CrossRef]
4. Davidovits, J. Geopolymers: Inorganic polymeric new materials. *J. Therm. Anal. Calorim.* **1991**, *37*, 1633–1656. [CrossRef]

5. Xu, H.; Van Deventer, J.S.J. Effect of source materials on geopolymerisation. *Eng. Chem. Res.* **2003**, *42*, 1698–1716. [CrossRef]
6. Luna-Galiano, Y.; Leiva, C.; Arenas, C.; Arroyo, F.; Vilches, L.F.; Villegas, R.; Fernández-Pereira, C. Behaviour of Fly Ash-Based Geopolymer Panels Under Fire. *Waste Biomass Valorization* **2017**, *8*, 2485–2494. [CrossRef]
7. Luna Galiano, Y.; Fernández Pereira, C.; Pérez, C.M.; Suarez, P. Influence of BFS content in the mechanical properties and acid attack resistance of fly ash based geopolymers. *Key Eng.* **2016**, *663*, 50–61. [CrossRef]
8. Lu, N.; Ran, X.; Pan, Z.; Korayem, A.H. Use of Municipal Solid Waste Incineration Fly Ash in Geopolymer Masonry Mortar Manufacturing. *Materials* **2022**, *15*, 8689. [CrossRef]
9. Zhao, Y.; Yang, C.; Yan, C.; Yang, J.; Wu, Z. Design and Properties of Coal Gangue-Based Geopolymer Mortar. *Buildings* **2022**, *12*, 1932. [CrossRef]
10. Andreola, F.; Barbieri, L.; Lancellotti, I.; Bignozzi, M.C.; Sandrolini, F. New blended cement from polishing and grazing ceramic sludge. *Int. J. Appl. Ceram.* **2010**, *7*, 546–555. [CrossRef]
11. Lancellotti, I.; Kamseu, E.; Michelazzi, M.; Barbieri, L.; Corradi, A.; Leonelli, C. Chemical stability of geopolymers containing municipal solid waste incinerator fly ash. *Waste Manag.* **2010**, *30*, 673–679. [CrossRef]
12. Rapazote, J.G.; Laginhas, C.; Teixeira-Pinto, A. Developed of building materials through alkaline activation of construction and demolition waste (CDW)-Resistance to acid attack. *Adv. Sci. Technol.* **2010**, *69*, 159–163. [CrossRef]
13. Vaou, V.; Panias, D. Thermal insulating foamy geopolymers from perlite. *Miner. Eng.* **2010**, *23*, 1146–1151. [CrossRef]
14. Tripathy, S.K.; Dasu, J.; Murthy, Y.R.; Kapure, G.; Pal, A.R.; Filippov, L.O. Utilization perspective on water quenched and air-cooled blast furnace slags. *J. Clean. Prod.* **2020**, *262*, 121354. [CrossRef]
15. Ríos, J.D.; Vahí, A.; Leiva, C.; Martínez-De la Concha, A.M.; Cifuentes, H. Analysis of the utilization of air-cooled blast furnace slag as industrial waste aggregates in self-compacting concrete. *Sustainability* **2019**, *11*, 1702. [CrossRef]
16. Ríos, J.D.; Arenas, C.; Cifuentes, H.; Vilches, L.F.; Leiva, C. Development of a paste for passive fire protection mainly composed of granulated blast furnace slag. *Environ. Prog. Sustain. Energy* **2020**, *39*, e13382. [CrossRef]
17. Azad, N.M.; Samarakoon, S.M.S.M.K. Utilization of Industrial By-Products/Waste to Manufacture Geopolymer Cement/Concrete. *Sustainability* **2021**, *13*, 873. [CrossRef]
18. Abdel-Ghania, N.T.; El-Sayedb, H.A.; El-Habak, A.A. Utilization of by-pass cement kiln dust and air-cooled blast-furnace steel slag in the production of some "green" cement products. *HBRC J.* **2018**, *14*, 408–414. [CrossRef]
19. Tole, I.; Rajczakowska, M.; Humad, A.; Kothari, A.; Cwirzen, A. Geopolymer Based on Mechanically Activated Air-cooled Blast Furnace Slag. *Materials* **2020**, *13*, 1134. [CrossRef] [PubMed]
20. Ahn, B.-H.; Lee, S.-J.; Park, C.-G. Physical and Mechanical Properties of Rural-Road Pavement Concrete in South Korea Containing Air-Cooled Blast-Furnace Slag Aggregates. *Appl. Sci.* **2021**, *11*, 5645. [CrossRef]
21. Arenas, C.; Ríos, J.D.; Cifuentes, H.; Vilches, L.F.; Leiva, C. Sound absorbing porous concretes composed of different solid wastes. *Eur. J. Environ. Civ. Eng* **2020**, *26*, 3805–3817. [CrossRef]
22. Skevi, L.; Baki, V.A.; Feng, Y.; Valderrabano, M.; Ke, X. Biomass Bottom Ash as Supplementary Cementitious Material: The Effect of Mechanochemical Pre-Treatment and Mineral Carbonation. *Materials* **2022**, *15*, 8357. [CrossRef]
23. Pérez-Villarejo, L.; Eliche-Quesada, D.; Carrasco-Hurtado, B.; Sánchez-Soto, P.J. Valorization of Olive Biomass Fly Ash for Production Eco Friendly Ceramic Bricks. *Encycl. Renew. Sustain. Mater.* **2020**, *5*, 285–294. [CrossRef]
24. Eliche-Quesada, J.; Leite-Costa, J. Use of bottom ash from olive pomace combustion in the production of eco-friendly fired clay bricks. *Waste Manag.* **2016**, *48*, 323–333. [CrossRef]
25. Rosales, M.; Rosales, J.; Agrela, F.; de Rojas, M.I.S.; Cabrera, M. Design of a new eco-hybrid cement for concrete pavement, made with processed mixed recycled aggregates and olive biomass bottom ash as supplementary cement materials. *Constr. Build. Mater.* **2022**, *358*, 129417. [CrossRef]
26. Peceño, B.; Hurtado-Bermudez, S.; Alonso-Fariñas, B.; Villa-Alfageme, M.; Más, J.L.; Leiva, C. Recycling Bio-Based Wastes into Road-Base Binder: Mechanical, Leaching, and Radiological Implications. *Appl. Sci.* **2023**, *13*, 1644. [CrossRef]
27. Cabrera, M.; Díaz-López, J.L.; Agrela, F.; Rosales, J. Eco-Efficient Cement-Based Materials Using Biomass Bottom Ash: A Review. *Appl. Sci.* **2020**, *10*, 8026. [CrossRef]
28. Beltrán, M.G.; Barbudo, A.; Agrela, F.; Jiménez, J.R.; de Brito, J. Mechanical performance of bedding mortars made with olive biomass bottom ash. *Constr. Build. Mater.* **2016**, *112*, 699–707. [CrossRef]
29. Leiva, C.; Gómez-Barea, A.; Vilches, L.F.; Ollero, P.; Vale, J.; Fernández-Pereira, C. Use of biomass gasification fly ash in lightweight plasterboard. *Energy Fuels* **2007**, *21*, 361–367. [CrossRef]
30. Nogales, R.; Delgado, G.; Quirantes, M.; Romero, M.; Romero, E.; Molina-Alcaide, E. Characterization of Olive Waste Ashes as Fertilizers. In *Recycling of Biomass Ashes*; Insam, H., Knapp, B., Eds.; Springer: Berlin/Heidelberg, Germany, 2011. [CrossRef]
31. *EN 196-1*; Methods of Testing Cement—Part 1: Determination of Strength. Spanish Association for Standardization and Certification: Madrid, Spain, 2018.
32. Available online: http://www.icdd.com (accessed on 16 May 2023).
33. Gates-Rector, S.; Blanton, T. The Powder Diffraction File: A quality materials characterization database. *Powder Diffr.* **2019**, *34*, 352–360. [CrossRef]
34. El-Mir, A.; El-Hassan, H.; El-Dieb, A.; Alsallamin, A. Development and Optimization of Geopolymers Made with Desert Dune Sand and Blast Furnace Slag. *Sustainability* **2022**, *14*, 7845. [CrossRef]

35. *EN 1936*; Natural Stone Test Methods—Determination of Real Density and Apparent Density, and of Total and Open Porosity. Spanish Association for Standardization and Certification: Madrid, Spain, 2007.
36. *EN 1015-11*; Methods of Test for Mortar for Masonry—Part 11: Determination of Flexural and Compressive Strength of Hardened Mortar. Spanish Association for Standardization and Certification: Madrid, Spain, 2020.
37. Leiva, C.; Arenas, L.F.V.; Vilches, L.F.; Arroyo, F.; Luna-Galiano, Y. Assessing durability properties of noise barriers made of concrete incorporating bottom ash as aggregates. *Eur. J. Environ. Civ. Eng.* **2019**, *23*, 1485–1496. [CrossRef]
38. *EN 998-2*; Specification for Mortar for Masonry—Part 2: Masonry Mortar. Spanish Association for Standardization and Certification: Madrid, Spain, 2018.
39. *EN 12457-4*; Characterisation of Waste—Leaching—Compliance Test for Leaching of Granular Waste Materials and Sludges—Part 4: One Stage Batch Test at a Liquid to Solid Ratio of 10 l/kg for Materials with Particle Size below 10 mm (without or with Size Reduction). Spanish Association for Standardization and Certification: Madrid, Spain, 2003.
40. US EPA. Toxicity Characteristics Leaching Procedure, Method 1311. Test Methods for the Evaluation of Solid Waste. 1992. Available online: https://www.epa.gov/sites/default/files/2015-12/documents/1311.pd (accessed on 10 March 2023).
41. *NEN 7375*; Leaching Characteristics—Determination of the Leaching of Inorganic Components from Moulded or Monolitic Materials with a Diffusion Test—Solid Earthy and Stony Materials. NEN (Netherlands Standardization Institute): Delf, The Netherlands, 2005.
42. US EPA. Method 1315: Mass Transfer Rates of Constituents in Monolithic or Compacted Granular Materials Using a Semi-Dynamic Tank Leaching Procedure. In *Test Methods for Evaluating Solid Waste, Physical/Chemical Methods*; US Environmental Protection Agency: Washington, DC, USA, 1986.
43. Council Directive 1999/31/EC of 26 April 1999 on the landfill of Waste. Official Journal L 182, 16/07/1999 P. 0001–0019. European Commission, 1999. Available online: http://data.europa.eu/eli/dir/1999/31/oj (accessed on 8 March 2022).
44. *DL 183/2009*; Waste Disposal at Landfills. Transposition to the Portuguese Law of Council. Directive 1999/31/CE, April 26. Portuguese Official Journal, Portuguese Mint and Official Printing Office: Lisbon, Portugal, 2009.
45. Ministero dell'Ambiente e Della Tutela Del Territorio. Decreto 5 Aprile 2006, n 186. Regolamento Recante Modifiche al Decreto Ministeriale 5 Febbraio 1998 «Individuazione Dei Rifiuti Non Pericolosi Sottoposti Alle Procedure Semplificate Di Recupero, ai Sensi Degli Articoli 31 e 33 Del Decreto Legislativo 5 Febbraio 1997, n. 22». Gazzeta Ufficiale, GU Serie Generale n.115 Del 19-05-2006, Italia, Roma. 2006. Available online: https://www.gazzettaufficiale.it/eli/id/2006/05/19/006G0202/sg (accessed on 10 March 2023).
46. Decreto 100/2018 de Valorización de Escorias en la Comunidad Autónoma de Cantabria. Cantabria, Spain, 2019. Available online: https://boc.cantabria.es/boces/verAnuncioAction.do?idAnuBlob=333876 (accessed on 8 March 2022).
47. Decreto 34 del País Vasco por el que se Regula la Valorización y Posterior Utilización de Escorias Procedentes de la Fabricación de Acero en Hornos de arco Eléctrico, en el Ámbito de la Comunidad Autónoma del País Vasco. País Vasco, Spain, 2003. Available online: https://www.legegunea.euskadi.eus/eli/es-pv/d/2003/02/18/34/dof/spa/html/webleg00-contfich/es/ (accessed on 8 March 2022).
48. Soares, I.; Nobre, F.X.; Vasconcelos, R.; Ramírez, M.A. Study of Metakaolinite Geopolymeric Mortar with Plastic Waste Replacing the Sand: Effects on the Mechanical Properties, Microstructure, and Efflorescence. *Materials* **2022**, *15*, 8626. [CrossRef] [PubMed]
49. *ASTM C270-19*; Standard Specification for Mortar for Unit Masonry. ASTM International: West Conshohocken, PA, USA, 2019.